Electronic Supplementary Material (ESI) for Chemical Communications.

Supporting Information

Decomposition of P_4O_{10} in DMSO

Sebastian Johansson[a], Christopher Kuhlmann[b], Johannes Weber[a], Thomas Paululat[c], Carsten Engelhard[b] and Jörn Schmedt auf der Günne*[a]

Abstract: The oxidation power of activated dimethyl sulfoxide (DMSO) with phosphorus pentoxide, better known as Onodera reagent[1], is not yet understood. Possible intermediates were studied in this manuscript. We found that DMSO is not dissolving P_4O_{1O}, but rather reacting with it. The system was studied with ^{31}P, $^{31}P\{^1H\}$ single excitation NMR, $^{31}P\{^1H\}$ correlation (COSY) NMR and high-resolution mass spectrometry. The findings are supported by $^{31}P\{^1H\}$ and ^{31}P NMR simulations, performed using the program SIMPSON[2]. We found that a rather complex mixture of phosphate species is formed, many with ester function. We explain the findings by a pummerer like transposition when the nucleophilic oxygen of the DMSO attacks the electrophilic phosphorus atom of the phosphorus pentoxide. The suggestion of a molecule occurring as intermediate, $C_2H_5S^+$, could be supported by high-resolution mass spectrometry. Its most stable conformation has been found by DFT calculations. Finally, we present a possible reaction mechanism for the decomposition of P_4O_{10} in DMSO. Finally, we present a possible decomposition scheme of P_4O_{10} in DMSO.

DOI: 10.1039/C8CC03000F

[a] S. Johansson, Dr. J. Weber, Prof. Dr. J. Schmedt auf der Günne
Inorganic Materials Chemistry, Department of Chemistry and Biology
University of Siegen, Adolf-Reichwein-Str. 2, 57076 Siegen, Germany, E-mail: gunnej@chemie.uni-siegen.de
[b] C. Kuhlmann, Prof. Dr. C. Engelhard
Department of Chemistry and Biology
University of Siegen, Adolf-Reichwein-Str. 2, 57076 Siegen, Germany
[c] Dr. T. Paululat
Department of Chemistry and Biology
University of Siegen, Adolf-Reichwein-Str. 2, 57076 Siegen, Germany

Table of Contents

1. Experimental Procedures

Handling the samples

In order to try to prevent water entering the reaction, a series of measures were taken. A high-purity batch of DMSO was bought. This was additionally dried with freshly preheated molecular sieve and all samples and the DMSO were handled in Schlenk flasks which we additionally dried under vacuum with a heat gun. Sample handling where necessary included a glove box. The Ar used was purified using several reagents including P_4O_{10} and Ti-sponge. Used syringes and flasks were flushed with Ar and evacuated several times before usage. The reagent P_4O_{10} was coming from a fresh high-grade batch. Its container was partially opened in a desiccator, immediately transferred into a glove box and remained there. Because of ^{1}H NMR experiments, which were done earlier and which allow to trace even small quantities of water, we were confident that the anhydrous grades could be trusted. Even small amounts of water are visible from ^{1}H NMR experiments.

NMR: ^{31}P and ^{31}P{^{1}H} spectroscopy

Single pulse and decoupled spectra were measured on a JEOL Eclipse EX-270 spectrometer with standard pulse sequences. 1% TMS in $CDCl_3$ was used as external reference. 0.5 mmol (141.9 mg) phosphorus pentoxide (Riedel de Haën, 99%) was dissolved in 1 mL DMSO.

NMR: ^{31}P correlation spectroscopy

The COSY spectrum was measured on a Varian VNMR-S 600 MHz spectrometer equipped with a 5 mm dual broadband probe. Pulse sequences were taken from Varian pulse sequence library. These spectra are recorded in 150µl of solvent at T = 25°C (T = 35°C for DMSO-d_6, Pyridine-d_5). Spectra are referenced with respect to external H_3PO_4. 1.5 mmol (425.8 mg) phosphorus pentoxide (Sigma-Aldrich, 99.98%) was dissolved in 3 mL d_6-DMSO.

Mass spectrometry

High-resolution mass spectrometric analysis was performed with an Exactive mass spectrometer (Thermo Fisher Scientific Inc., Bremen, Germany). The conventional inlet capillary was replaced by a 4 cm extended stainless-steel capillary (i.d. 0.8 mm, o.d. 1.58 mm). For direct sample desorption/ionization a home-built FAPA source (pin-to-capillary geometry, described by Shelley *et al.*[1]) powered by a model BHK 1000-0.2MG DC power supply (Kepco Inc., Flushing, NY, USA) was used. A negative potential (25 mA, 705 V) was applied to the stainless-steel pin electrode with a 5 kW ballast resistor as part of the circuitry. The stainless-steel capillary anode was connected to ground potential of the power supply. Helium (99.999%, Messer Industriegase GmbH, Siegen, Germany) was used as discharge gas. It was fed through an additional port with 500 mL min^{-1} into the ceramic discharge chamber made out of Macor (Schröder Spezialglas GmbH, Ellerau, Germany). The FAPA was positioned on-axis in front of the MS inlet capillary with a distance of 7 mm. For sample analysis, 0.5 µL of the reaction mixture was deposited on a stainless-steel metal mesh at ambient conditions. The prepared sample was positioned between the FAPA source and the MS inlet capillary at a distance of 1 mm towards the MS inlet capillary. A schematic diagram of this experimental setup can be found in Figure S3.

Background signals (ambient air etc.) were subtracted from the mass spectra by using the “subtract background” function of the vendor data processing software Xcalibur (Thermo Fisher Scientific Inc., Bremen, Germany).

Quantum-chemical calculations

All calculations were performed using Gaussian 09 at either HF/6-31G(d,p) level [3,4] or hybrid DFT level (PBE1PBE [5–7]) with aug-cc-pVTZ [8] basis set. Tight convergence criteria were set for the SCF cycles (scf=tight, corresponding to $\Delta E<10^{-8}$ hartree and a change in the density matrix elements < 10^{-8} in subsequent steps), as well as the structure optimization (opt=tight, corresponding to a combined criterion of the scf=tight condition, and maximum residual forces and displacements on individual atoms of 0.000015 hartree/bohr and 0.000060 bohr, respectively. On RMS average over all nuclei these quantities were not allowed to be larger then 0.000010 hartree/bohr and 0.000040 bohr). In the DFT calculation the “ultrafine” integration grid was used, corresponding to pruned grid of 99 radial shells and 590 angular points per shell on each atom. This combination should lead to reliable structures as well as relative energies [9]. At the converged structures, harmonic frequencies using analytic second derivatives [10] were calculated to prove that the optimized structure belongs to a local minimum on the potential energy surface and to obtain the total energy of the molecule. The zero point energy was added to the electronic energy, and thermal corrections were included by thermal populations of the harmonic levels according to [11] with a special treatment of soft vibrations that might belong to internal rotations according to Truhlar *et al.* (keyword: freq=HindRot) [12–14]. For HF/6-31G** frequencies a scaling of 0.89 was used, while no factor was used for the DFT frequencies.

NMR simulations

The program SIMPSON[2] was used to perform simulations. An offset of -5580 Hz was applied to every simulation by manually moving the chemical shifts. This was done in order to be able to maintain the sw parameter from the experiment

2. Results and Discussion

2.1. Mass spectrometry

In Figure S1, the mass spectrum of pure DMSO detected by FAPA-MS is depicted. The mass spectrum does not contain a peak at *m*/*z* 61.01073, which would correspond to the $C_2H_5S^+$ cation (MA 1.4 ppm) found in the Onodera reagent (see Figure 1B). This finding confirms that $C_2H_5S^+$ is not formed during the desorption/ionization process by the FAPA source.

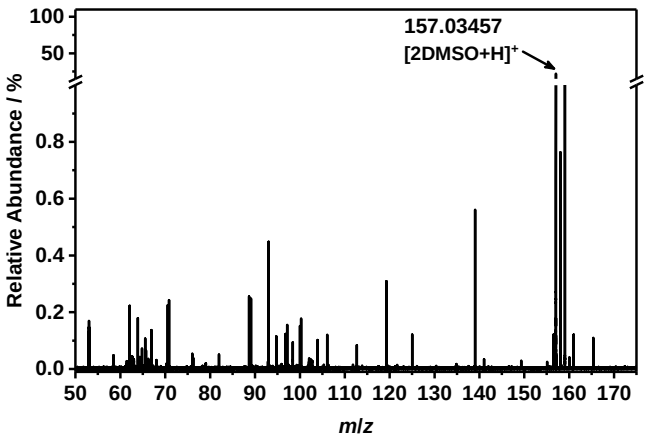

Figure S1. Mass spectrum of pure DMSO in the mass range between *m*/*z* 50 and 150 detected by FAPA-MS in positive-ion mode. For visualization purposes the peak height was normalized to the largest peak (*m*/*z* 157) in Figure 5B.

In negative-ion mode FAPA-MS analysis of the Onodera reagent, multiple phosphate- and sulphate-species can be observed due to possible oxidation processes inside the reaction mixture, at ambient conditions, or the exposure of the analyte to the plasma source. A list of all peaks at different *m*/*z* is provided in Table S1 and a corresponding mass spectrum is depicted in Figure S2.

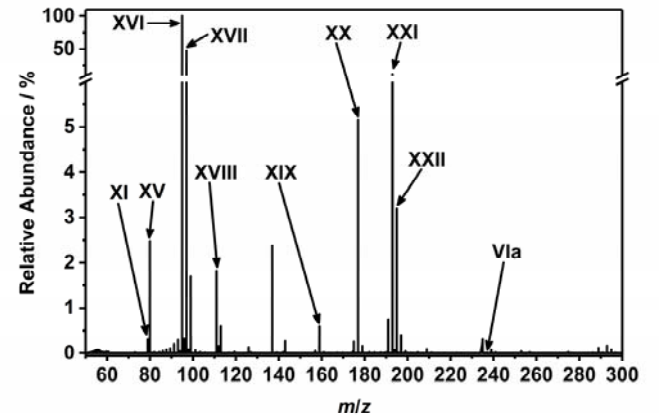

Figure S2. Mass spectrum of the P_4O_{10}-DMSO mixture detected by FAPA-MS in negative-ion mode (mass accuracy limit for peak identification ≤ +/-15 ppm).

Table S1. List of identified peaks in the mass spectrum of the P_4O_{10}-DMSO mixture detected by FAPA-MS (negative-ion mode).

No.	Observed *m*/*z*	Sum formula	Theoretical mass	Relative mass accuracy
XI	78.95811	$O_{12}P_4^{4-}$	78.95905	-11.3 ppm
XV	79.95648	O_3S^-	79.95736	-11.0 ppm
XVI	94.97986	$CH_3SO_3^-$	94.98084	-10.3 ppm
XVII	96.95914	SO_4H^-	96.96010	-9.9 ppm
XVIII	110.97471	$CH_3O_4S^-$	110.97575	-9.4 ppm
XIX	158.91459	O_6PS^-	158.91587	-8.1 ppm
XX	176.92536	$H_2O_7PS^-$	176.92643	-6.1 ppm
XXI	192.95663	$CH_6O_7PS^-$	192.95773	-5.7 ppm
XXII	194.93596	$H_4O_8PS^-$	194.93700	-5.3 ppm
VIa	236.93585	$C_2H_7O_7P_2S^-$	236.93932	-14.7 ppm

In Figure S3 the experimental setup of transmission-mode FAPA-MS is depicted. The FAPA source was positioned on-axis in front of the inlet capillary of the mass spectrometer with a distance of 7 mm. The distance between stainless-steel mesh and MS inlet capillary was 1 mm.

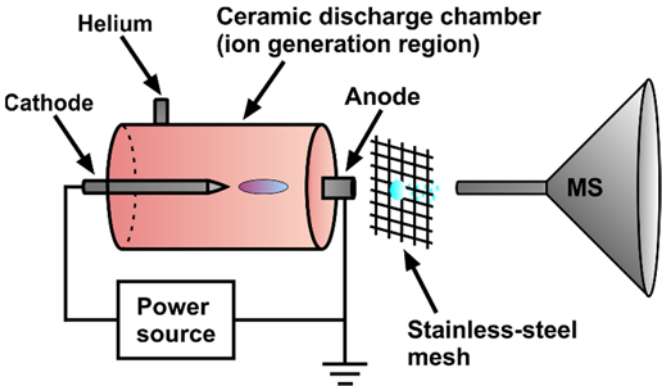

Figure S3. Instrumental setup of transmission-mode FAPA-MS.

2.2. ^{31}P-COSY simulations

Besides the μ-oxido-cyclotetraphosphate anion – substance XIII, spin system A_2X_2 - two more phosphates could be identified, both being ortho-phosphono-tricyclophosphate anions. In the case of substance XII, the two Q^2 phosphorus atoms are anisochronous, while in substance XIV these atoms are isochronous. The sum projections of the COSY spectrum can be seen in **Figure S4** and **Figure S5**.

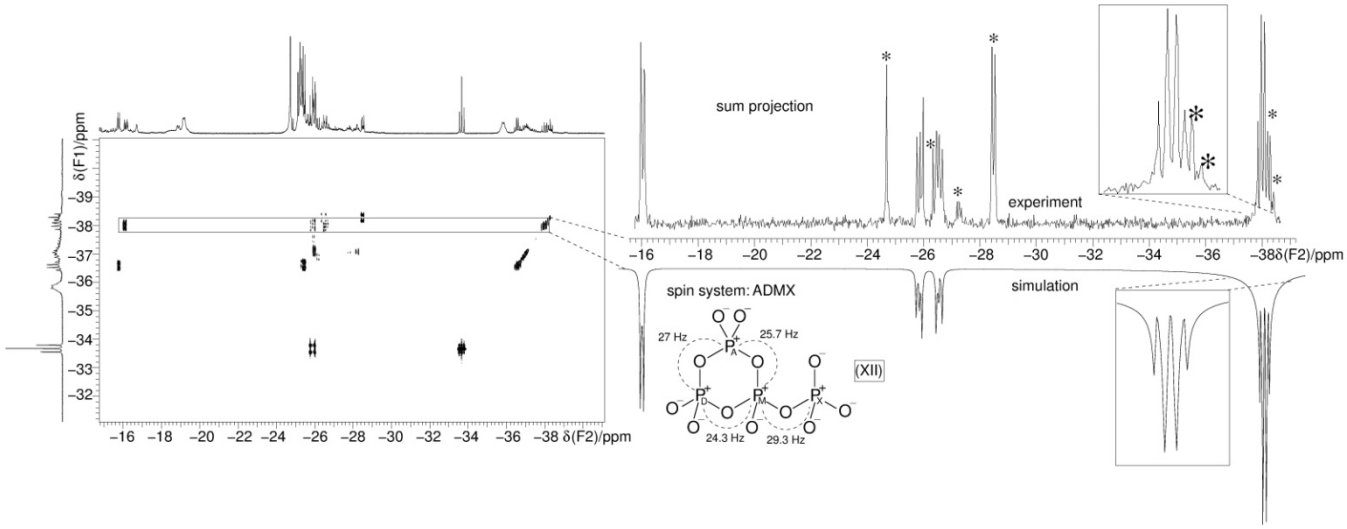

Figure S4: Zoom in of a ^{31}P COSY spectrum (middle). On the x and y axis ^{31}P single excitation spectra are shown. On the right top the sum projection of the section from the COSY spectrum surrounded by the box is shown versus a simulated sum projection. On the left top a zoom in the section is shown versus the simulation of the COSY spectrum of the ortho-phosphono-tricyclophosphate anion with ADMX spin system. The found J-couplings are depicted in the figure. Asterixes in the experimental sum projection mark peaks from other phosphate species, coming from overlapping signals in the 2D spectrum.

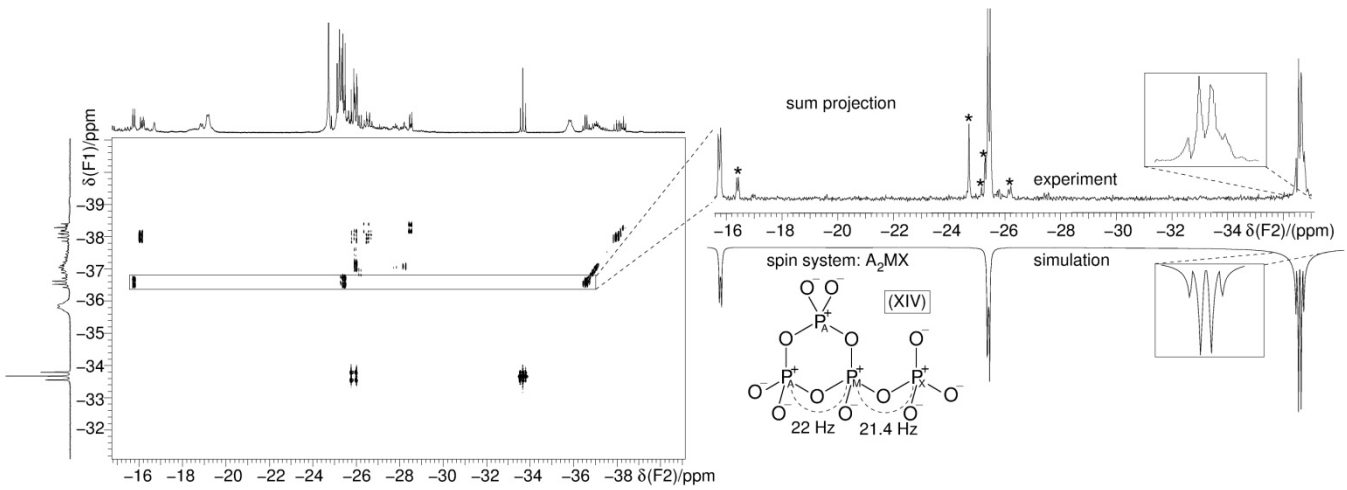

Figure S5: Zoom in of a ^{31}P COSY spectrum (middle). On the x and y axis ^{31}P single excitation spectra are shown. On the right top the sum projection of the section from the COSY spectrum surrounded by the box is shown versus a simulated sum projection. On the left top a zoom in the section is shown versus the simulation of the COSY spectrum of another ortho-phosphono-tricyclophosphate anion with A_2MX spin system. The found J-couplings are depicted in the figure. Asterixes in the experimental sum projection mark peaks from other phosphate species, coming from overlapping signals in the 2D spectrum.

2.3. Quantumchemical calculations

Table S2. Results of the calculations at HF/6-31G(d,p) level. ΔE_{total} is the total enery difference between the present and the lowest energetic isomer.

Molecule	E(HF/6-31G(d,p))	ZPE(HF)	Thermal correction[a] to H_f at T=			Hindered rotor correction, T=			ΔE_{total}	ΔE_{total}	ΔE_{total}	Symmetry
			298.15K=25° C	430K=157° C	500K=227°C	@298.15K	@430K	@500K	@298.15K	@430K	@500K	
	in a.u.	kJ/mol	kJ/mol	kJ/mol	kJ/mol	kJ/mol	kJ/mol	kJ/mol	kJ/mol	kJ/mol	kJ/mol	
$C_2H_5S^+$	-475.71054	169.37	15.14	26.44	33.39	0	0	-0.004	415.88	419.13	415.88	C_2
cyclo-$C_2H_5S^+$	-475.87315	183.3	12.25	20.3	25.96	0	0	0	0	0	0	C_s
H_2C-S-CH_3^+	-475.871	180.81	14.6	26.18	32.72	-3.694	-4.523	-4.895	1.799233	4.5002	1.80	C_s
t-$C_2H5_S^+$	-475.79086	158.1	17.17	30.53	38.02	-2.276	-3.791	-4.548	193.4875	197.28	193.48	C_2
t-cyclo-$C_2H5_S^+$	-475.63501	163.04	15.37	28.04	35.19	0	0	0	608.075	612.695	608.07	C_1
t-H_2C-S-CH_3^+	-475.82411	169.95	15.41	27.64	34.58	-0.854	-1.527	-1.883	117.698	121.205	117.69	C_s

[a] a scaling factor of 0.89286 was included

Table S3. Results of the DFT calculations at PBE1PBE/aug-cc-pVTZ level. ΔE_{total} is the total enery difference between the present and the lowest energetic isomer.

Molecule	E(PBE1PBE/ aug-cc-VTZ)	ZPE(DFT)	Thermal correction to H_f at T=			Hindered rotor correction, T=			ΔE_{total}	ΔE_{total}	ΔE_{total}	Symmetry
			298.15K=25°C	430=157°C	500K=227°C	298.15K	430K	500K	@298K	@430K	@500K	
	in a.u.	kJ/mol	kJ/mol	kJ/mol	kJ/mol	kJ/mol	kJ/mol	kJ/mol	kJ/mol	kJ/mol	kJ/mol	
$C_2H_5S^+$	-476.78829	155.53	15.78	27.23	34.23	-0.013	-0.063	-0.1	315.16	317.29	318.22	C_2
cyclo-$C_2H_5S^+$	-476.91272	170.89	11.93	21.2	27.23	0	0	0	0.00	0.00	0.00	C_s
H_2C-S-CH_3^+	-476.90468	168.71	14.18	24.11	30.36	-2.556	-3.473	-3.887	18.62	18.36	18.17	C_s
t-$C_2H5_S^+$	-476.79251	149.09	16.77	28.85	36.15	-1.477	-2.565	-3.138	297.18	298.91	299.60	C_1 (!)
t-cyclo-$C_2H5_S^+$	-476.79251	149.09	16.77	28.85	36.15	-1.477	-2.565	-3.138	297.18	298.91	299.60	C_1(ring opening)
t-H_2C-S-CH_3^+	-476.83018	158.53	15.46	26.65	33.49	-0.866	-1.548	-1.9	207.02	208.26	208.72	C_s

The optimized structures are shown in Fig. S6.

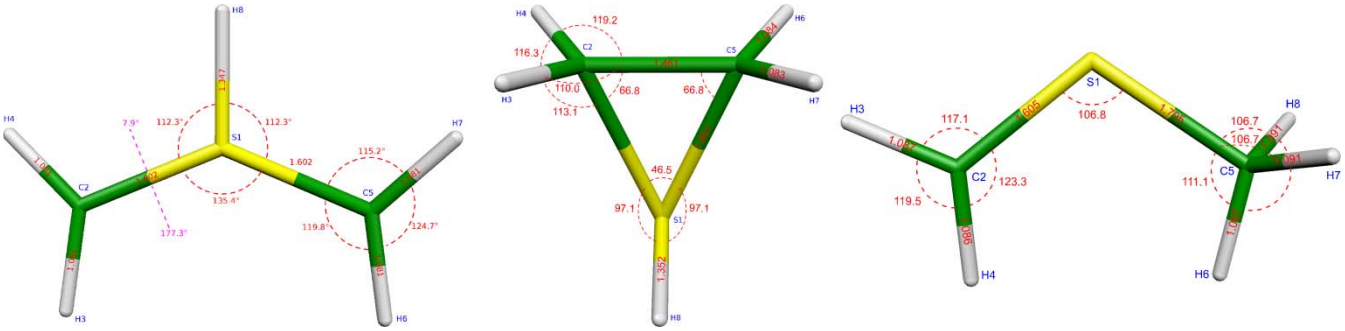

(a) **(b)** **(c)**

Figure S6. Optimized Structures on DFT (PBE1PBE/aug-cc-pVTZ) level. (a) $C_2H_5S^+$, (b) cyclo-$C_2H_5S^+$, (c) H_2C-S-CH_3^+

2.4. SIMPSON input files
2.4.1 2D COSY simulation for Substance XII

```
spinsys {
  channels 31P
  nuclei 31P 31P 31P 31P
  jcoupling 1 2  25.7 0 0 0 0 0
  jcoupling 2 3  27    0 0 0 0 0
  jcoupling 1 3  24.3 0 0 0 0 0
  jcoupling 1 4  29.3 0 0 0 0 0
  shift 1 -3651 0 0 0 0 0
  shift 2 -857 0 0 0 0 0
  shift 3 -687 0 0 0 0 0
  shift 4 1693 0 0 0 0 0

}

par {
  proton_frequency     600e6
  method               direct
  spin_rate            0
  gamma_angles         1
  crystal_file         alpha0beta0
  np                   4096
  ni                   512
  variable  si         4096
  start_operator       Inz
  detect_operator      Inp
  verbose              11111111111111
  sw                   13665
  sw1                  11160
  variable lb          6
  variable resolution  0.0
}

proc pulseq {} {
  global par spinsys

  #DQ-Filter
  matrix set 1 totalcoherence {+1}
  matrix set 2 totalcoherence {0}

#----evolution in t2 ------
  reset
  delay [expr 1.0e6/$par(sw)]
  store 2

#---evolution in t1 -----
  reset
  delay [expr 1.0e6/$par(sw1)]
  store 1

#----core program -----

  for {set i 0} {$i < $par(ni)} {incr i 2} {

    foreach ph {0.0 90.0} {
      reset

      pulseid 1 250000 $ph
      prop 1 [expr {$i/2}]
      filter 1
      pulseid 1 250000 90
      acq $par(np) 2
```

```
    }
  }
}
proc main {} {
  global par spinsys

# ------ start powder loop ------
  set f [fsimpson]

  fzerofill $f $par(si) $par(si)
  faddlb $f $par(lb) 0 $par(lb) 0 -phsens
  fft $f 0 0 0 0 -phsens


  for {set i 1} {$i <= $par(si)} {incr i} {
    for {set j 1} {$j <= $par(si)} {incr j} {
      set old [findex $f $i $j]
      set re [lindex $old 0]
      set im [lindex $old 1]
      fsetindex $f $i $j [expr {sqrt($re*$re+$im*$im)}] 0.0
    }
  }
  fsave $f $par(name).spe -gnu2d
  funload $f
}
```

2.4.2 2D COSY simulation SIMPSON input file Substance XIII – Spin system part only

```
spinsys {
  channels 31P
  nuclei 31P 31P 31P 31P
  jcoupling 1 2  29.15 0 0 0 0 0
  jcoupling 1 3  29.15 0 0 0 0 0
  jcoupling 2 4  29.15 0 0 0 0 0
  jcoupling 3 4  29.15 0 0 0 0 0
  shift 1 -639 0 0 0 0 0
  shift 2 -2582 0 0 0 0 0
  shift 4 -639 0 0 0 0 0
  shift 3 -2582 0 0 0 0 0
}
```

2.4.3 2D COSY simulation SIMPSON input file Substance XIV – Spin system part only

```
spinsys {
  channels 31P
  nuclei 31P 31P 31P 31P

  jcoupling 1 2  22 0 0 0 0 0
  jcoupling 1 3  22 0 0 0 0 0
  jcoupling 1 4  21.4 0 0 0 0 0

  shift 1 -3311 0 0 0 0 0
  shift 2 -566 0 0 0 0 0
  shift 3 -566 0 0 0 0 0
  shift 4 1766 0 0 0 0 0
}
```

2.4.4. Gnuplot script for plotting 2D COSY spectrum of Substance XIII

```
set title "2D contourplot"
unset surface
```

```
set timestamp "%Y-%m-%d"
set contour
set cntrparam levels discrete 710000,540000,360000,240000,160000,130000
set view 0,90,1
set xlabel "SQ(F1)/ppm"
set ylabel "DQ(F2)/ppm"
set yrange [-12:-2]
set xrange [-11:-10]
set size square
splot "cosy-magnitude.spe" u ($1/242.828):($2/242.828):3 w l
set term postscript eps enhanced solid color
set output "cosy.eps"
replot
```

2.5. Chemical information of phosphates identified by NMR

I: H_3PO_4: ^{31}P-NMR (270 MHz, DMSO, 25°C, TMS): δ_{iso}=0.44 ppm
II: $(OP)(O\text{-}CH_2R)_3$: ^{31}P-NMR (270 MHz, DMSO, 25°C, TMS): δ_{iso}=-3.7 ppm
III: $(O_2P)(O\text{-}CH_2R)_2$-anion: ^{31}P-NMR (270 MHz, DMSO, 25°C, TMS): δ_{iso}=-4.36 ppm
IV: $(O_3P)(O\text{-}CH_2R)^{2-}$-anion: ^{31}P-NMR (270 MHz, DMSO, 25°C, TMS): δ_{iso}=-4.56 ppm
V: $(RCH_2O)_2$-OP-O-PO_3-anion: ^{31}P-NMR (270 MHz, DMSO, 25°C, TMS): δ_{iso}=-10.79 ppm,
VI: $P_2O_7^{4-}$-anion: ^{31}P-NMR (270 MHz, DMSO, 25°C, TMS): δ_{iso}=-12,4 ppm
VII: (RCH_2O)-(PO_2)-O-PO_3-anion: ^{31}P-NMR (270 MHz, DMSO, 25°C, TMS): δ_{iso}= -13.54 ppm
VIII: Tetraphosphate-anion: ^{31}P-NMR (270 MHz, DMSO, 25°C, TMS): δ_{iso}=-15 ppm, δ_{iso}=-25.06 ppm
IX: PO_3-O-PO_2-O-PO_3-anion: ^{31}P-NMR (270 MHz, DMSO, 25°C, TMS): δ_{iso}=-15.87 ppm, δ_{iso}=-27.61 ppm
X: $(RCH_2O)_2OP$-O-$PO(OCH_2R)_2$: ^{31}P-NMR (270 MHz, DMSO, 25°C, TMS): δ_{iso}=-16.14 ppm ($^2J(^{31}P\text{-}^{31}P)$=22.8 Hz, $^3J(^1H\text{-}^1H)$ = 16.1 Hz)
XI: $P_4O_{12}^{4-}$-anion: ^{31}P-NMR (270 MHz, DMSO, 25°C, TMS): δ_{iso}= -24.5 ppm
XII: $(P_3O_9PO_3)^{4-}$-anion: ^{31}P-NMR (600 MHz, d_6-DMSO, 25°C, TMS): δ_{iso}=-38 ppm (q, $^2J(^{31}P_A\text{-}^{31}P_M)$=25.7 Hz, $^2J(^{31}P_M\text{-}^{31}P_X)$=29.3 Hz), $^2J(^{31}P_D\text{-}^{31}P_M)$=24.3 Hz), -26.5 ppm (t, $^2J(^{31}P_A\text{-}^{31}P_D)$=27 Hz, $^2J(^{31}P_A\text{-}^{31}P_M)$=25.7 Hz), -25.8 ppm (t, $^2J(^{31}P_A\text{-}^{31}P_D)$=27 Hz, $^2J(^{31}P_D\text{-}^{31}P_M)$=24.3 Hz), -16ppm (d, $^2J(^{31}P_M\text{-}^{31}P_X)$=29.3 Hz)
XIII: $P_4O_{11}^{2-}$-anion: ^{31}P-NMR (600 MHz, d_6-DMSO, 25°C, TMS): δ_{iso}=-33.6 ppm (t, $^2J(^{31}P_A\text{-}^{31}P_X)$=29.15 Hz), -25.6ppm (d, $^2J(^{31}P_A\text{-}^{31}P_X)$=29.15 Hz)
XIV: $(P_3O_9PO_3)^{4-}$-anion: ^{31}P-NMR (600 MHz, d_6-DMSO, 25°C, TMS): δ_{iso}=-36.6 ppm (q, $^2J(^{31}P_A\text{-}^{31}P_M)$=22 Hz, $^2J(^{31}P_M\text{-}^{31}P_X)$=21.4 Hz), -25.3 ppm (d, $^2J(^{31}P_A\text{-}^{31}P_M)$=22 Hz), -15.7 ppm (d, $^2J(^{31}P_M\text{-}^{31}P_X)$=21.4 Hz)

References

[1] K. Onodera, S. Hirano, N. Kashimura, *J. Am. Chem. Soc.* **1965**, *87*, 4651–4652.
[2] M. Bak, J. T. Rasmussen, N. C. Nielsen, *J. Magn. Reson.* **2000**, *147*, 296–330.
[3] P. C. Hariharan, J. A. Pople, *Theor. Chim. Acta* **1973**, *28*, 213–222.
[4] W. J. Hehre, R. Ditchfield, J. A. Pople, *J. Chem. Phys.* **1972**, *56*, 2257–2261.
[5] J. P. Perdew, K. Burke, M. Ernzerhof, *Phys. Rev. Lett.* **1996**, *77*, 3865–3868.
[6] J. P. Perdew, K. Burke, M. Ernzerhof, *Phys. Rev. Lett.* **1997**, *78*, 1396–1396.
[7] "G03 Manual: DFT," can be found under http://www.lct.jussieu.fr/manuels/Gaussian03/g_ur/k_dft.htm, **n.d.**
[8] T. H. Dunning, *J. Chem. Phys.* **1989**, *90*, 1007–1023.
[9] G. I. Csonka, A. Ruzsinszky, J. P. Perdew, *J. Phys. Chem. B* **2005**, *109*, 21471–21475.
[10] P. Pulay, *Adv. Chem. Phys.* **1987**, *69*, 241–286.
[11] D. A. McQuarrie, *Molecular Thermodynamics*, University Science Books, **1999**.
[12] Y.-Y. Chuang, D. G. Truhlar, *J. Chem. Phys.* **2000**, *112*, 1221–1228.
[13] Y.-Y. Chuang, D. G. Truhlar, *J. Chem. Phys.* **2004**, *121*, 7036–7036.
[14] Y.-Y. Chuang, D. G. Truhlar, *J. Chem. Phys.* **2006**, *124*, 179903.
[15] T. Glonek, J. R. Van Wazer, R. A. Kleps, T. C. Myers, *Inorg. Chem.* **1974**, *13*, 2337–2345.

Author Contributions

Sebastian Johansson:	writing of original draft, data curation, analysis of NMR measurements, NMR simulations (lead)
Christopher Kuhlmann:	mass spectrometry measurements and data analysis (supporting)
Dr. Johannes Weber:	DFT calculations (supporting)
Dr. Thomas Paululat:	measuring of ^{31}P-COSY-NMR (supporting)
Prof. Dr. Jörn Schmedt auf der Günne:	project administration, funding acquisition, analysis of NMR measurements, NMR simulations (lead)